

## 4-Substituted 1-Chloro-2-nitrobenzenes: Structure–Activity Relationships and Extension of the Substrate Model of Rat Glutathione *S*-Transferase 4-4

Ellen M. van der Aar,<sup>†</sup> Marcel J. de Groot,<sup>†,‡</sup> Tialda Bouwman,<sup>†</sup>  
Greetje J. Bijloo,<sup>†,‡</sup> Jan N. M. Commandeur,<sup>†</sup> and Nico P. E. Vermeulen<sup>\*,†</sup>

Leiden/Amsterdam Center for Drug Research, Department of Pharmacochimistry,  
Divisions of Molecular Toxicology and Medicinal Chemistry, Vrije Universiteit, De Boelelaan 1083,  
1081 HV Amsterdam, The Netherlands

Received August 1, 1996<sup>⊗</sup>

In the present study, eleven 4-substituted 1-chloro-2-nitrobenzenes were tested for their GSH conjugation capacity when catalyzed by base or rat glutathione *S*-transferase (GST) 4-4. Kinetic parameters ( $k_s$  and  $K_m$ ,  $k_{cat}$ , and  $k_{cat}/K_m$ ) were determined and subsequently used for the description of structure–activity relationships (SAR's). For this purpose, eight physicochemical parameters (electronic, steric, and lipophilic) of the substituents and five computer-calculated parameters of the substrates (charge distributions and several energy values) were used in regression analyses with the kinetic parameters. The obtained SAR's are compared with corresponding SAR's for the GSH conjugation of 2-substituted 1-chloro-4-nitrobenzenes, previously determined [Van der Aar *et al.* (1996) *Chem. Res. Toxicol.* **9**, 527–534]. The kinetic parameters of the 4-substituted 1-chloro-2-nitrobenzenes correlated well with the Hammett  $\sigma_p^-$  constant; the Hammett  $\sigma_p$  constant corrected for "through resonance", while the corresponding kinetic parameters of the 2-substituted 1-chloro-4-nitrobenzenes did not. The base- and GST 4-4-catalyzed GSH conjugation reactions of 2-substituted 1-chloro-4-nitrobenzenes depend to a different extent on the electronic properties of the *ortho* substituents, suggesting the involvement of different rate-limiting transition states. The base- and GST 4-4-catalyzed conjugation of 4-substituted 1-chloro-2-nitrobenzenes, however, showed a similar dependence on the electronic properties of the *para* substituents, indicating that these substrates are conjugated to GSH via a similar transition state. Multiple regression analyses revealed that, besides electronic interactions, also steric and lipophilic restrictions appeared to play an important role in the GST 4-4-catalyzed GSH conjugation of 4-substituted 1-chloro-2-nitrobenzenes. Finally, the 4-substituted 1-chloro-2-nitrobenzenes were also used to extend the previously described substrate model for GST 4-4 [De Groot *et al.* (1995) *Chem. Res. Toxicol.* **8**, 649–658], by which a specific steric restriction of substrates for GST 4-4 became clear.

### Introduction

The glutathione *S*-transferases (GSTs; EC 2.5.1.18)<sup>1</sup> constitute a family of enzymes that catalyze the addition of the tripeptide GSH to lipophilic substrates bearing electrophilic functional groups (1, 2). The cytosolic enzymes are dimeric proteins with subunits (22–27 kDa) that appear to be organized into at least five principal gene classes designated  $\alpha$ ,  $\mu$ ,  $\pi$  (3),  $\theta$  (4), and  $\sigma$  (5). Both homo- and heterodimeric enzymes are found within a

gene class, but intergene class heterodimers are not known. Each subunit contains a binding site for GSH (G-site) and a separate binding site for electrophilic substrates (H-site), and there have been considerable efforts to characterize the molecular structure of these binding sites. These approaches include site-directed mutagenesis (6, 7) and construction of chimeric protein subunits (8) as well as affinity labeling (9, 10), NMR spectroscopy (11), and high-resolution X-ray studies on crystals of GST isoenzymes (12–14).

Recently, molecular modeling techniques were used to derive a substrate model for rat GST 4-4, an isoenzyme of which a crystal structure has not been described yet (15). Information on regio- and stereoselective product formation of 20 substrates, covering structurally different classes of chemicals [aromatic diol epoxides, pyrene oxide, (aza)phenanthrene oxides, and aromatic chlorides] was used to construct a substrate model containing three interaction sites responsible for Lewis acid–Lewis base interactions (IS<sub>1</sub>, IS<sub>2</sub>, and IS<sub>3</sub>), as well as a region responsible for aromatic interactions (IS<sub>4</sub>) (Figure 1). These interaction sites in the substrates corresponded with hypothetical protein interaction sites (*p*IS<sub>1</sub>, *p*IS<sub>2</sub>, *p*IS<sub>3</sub>, and *p*IS<sub>4</sub>) in the active site of GST 4-4 (15).

Structure–activity relationships (SAR's) have also been used to characterize the mechanism of action and

\* To whom correspondence should be addressed (tel, +31 (0)20 444 7590; fax, +31 (0)20 444 7610; e-mail, vermeule@chem.vu.nl).

<sup>†</sup> Division of Molecular Toxicology.

<sup>‡</sup> Division of Medicinal Chemistry.

<sup>⊗</sup> Abstract published in *Advance ACS Abstracts*, April 1, 1997.

<sup>1</sup> Abbreviations: BPDE, benzo[*a*]pyrene 7,8-diol 9,10-epoxide; CDNB, 1-chloro-2,4-dinitrobenzene; CSD, Cambridge Structural Database; DMA, distributed multipole analysis; DMSO, dimethyl sulfoxide;  $E_{HOMO}$ , energy of the highest occupied molecular orbital;  $E_{LUMO}$ , energy of the lowest unoccupied molecular orbital; GAMESS-UK, Generalised Atomic and Molecular Electronic Structure System, UK version; GS<sup>-</sup>, glutathione anion; GS-conjugate, GSH conjugate; GSTs, glutathione *S*-transferases; IS, interaction site in the substrate, which interacts with a corresponding *p*IS in the enzyme;  $\lambda_{max}$ , maximal absorbance wavelength; MeS<sup>-</sup>, methanethiolate anion or model nucleophile for the thiolate anion of GSH; *p*IS, protein interaction site, responsible for interaction with a corresponding IS in the substrate; RHF, restricted Hartree–Fock; STO, Slater-type orbital; SAR's, structure–activity relationships; S<sub>N</sub>Ar, nucleophilic aromatic substitution; SV, split valence.

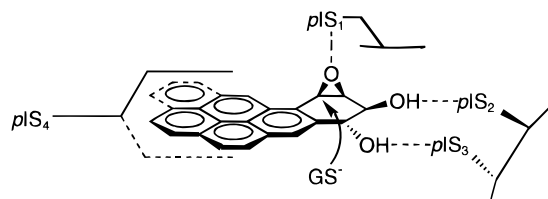


**Figure 1.** Substrate model for the active site of GST 4-4 with benzo[*a*]pyrene 7(*R*),8(*S*)-diol 9(*S*),10(*R*)-epoxide (BPDE) as the template (taken from 15). Epoxide oxygen atom ( $IS_1$ ), C<sub>8</sub>-hydroxyl group ( $IS_2$ ), and C<sub>7</sub>-hydroxyl group ( $IS_3$ ), interacting with protein interaction sites ( $pIS_1$ ,  $pIS_2$  and  $pIS_3$ , respectively), and aromatic interaction region ( $IS_4$ ) interacting with aromatic amino acids in the protein ( $pIS_4$ ).

the active sites of GSTs. Chemical variation of the structure of the cofactor GSH gave more insight in important interactions between GSH and amino acids in the G-site of GST 3-3 (16). The significance of hydrophobic and steric interactions in the active site of GSTs was explored by the determination of substrate specificities of 15 cytosolic GSTs from rat, human, and mouse by use of a homologous series of ten 4-hydroxyalkenals (17). Recently, Rietjens *et al.* described parallel SAR's for the overall rate of GSH conjugation of a series of five fluoronitrobenzenes when catalyzed by base and human and rat cytosolic GSTs (18, 19). For all catalysts, the interaction between the thiolate anion of GSH and the fluoronitrobenzene, leading to the Meisenheimer intermediates, is the rate-limiting step in overall conversion of this series of small substrates. Comparison of enzyme kinetic parameters of the GSH conjugation of eleven 2-substituted 1-chloro-4-nitrobenzenes, when catalyzed by rat GST isoenzymes of three different classes, showed major differences in the enzyme kinetic parameters and among others, in the GST isoenzyme selectivity (20). Recently, we also described SAR's for the GSH conjugation of a series of ten 2-substituted 1-chloro-4-nitrobenzenes catalyzed by base and by rat GST 4-4 (21). Steric, lipophilic, and electronic parameters were correlated with the kinetic parameters of the GSH conjugation reaction of these substrates. Moreover, charge distributions and several other molecular parameters were calculated for the substrates and the corresponding Meisenheimer intermediates with  $MeS^-$  as a model nucleophile for the thiolate anion of GSH and used in regression analyses. The comparison of SAR's for the base- and GST 4-4-catalyzed GSH conjugation reaction led, i.e., to the proposal that the rate-limiting transition states for the base-catalyzed and the GST 4-4-catalyzed GSH conjugation reaction are different (21).

In the present study the kinetic parameters of the base-catalyzed ( $k_c$ ) and GST 4-4-catalyzed ( $K_m$ ,  $k_{cat}$ , and  $k_{cat}/K_m$ ) GSH conjugation of eleven 4-substituted 1-chloro-2-nitrobenzenes (Table 1) are determined, compared, and described in terms of SAR's using eight classical physicochemical parameters and five computer-calculated molecular parameters of the substrates. The obtained SAR's were compared with SAR's for the base- and the GST 4-4-catalyzed GSH conjugation of 2-substituted 1-chloro-4-nitrobenzenes (Table 1), determined in a previous study (21). These SAR equations and their differences gave more detailed information about the active site of GST 4-4 and which interactions (electronic, steric, lipophilic) are important for the GSH conjugation of these substrates by GST 4-4. Also the previously reported substrate model for rat GST 4-4 (15) is refined by including the present series of 4-substituted 1-chloro-2-

nitrobenzenes, by which the steric restrictions of substrates for GST 4-4 became more clear.

## Experimental Procedures

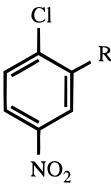
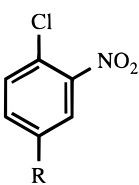
**Materials and Chemicals.** GSH was obtained from Boehringer (Mannheim, Germany), and 4-chloro-3-nitrobenzaldehyde (**2b**; 97% pure), 4-chloro-3-nitrobenzophenone (**3b**; 99% pure), 1-chloro-2-nitro-4-trifluoromethylbenzene (**8b**; 98% pure), and 1,4-dichloro-2-nitrobenzene (**9b**; 99% pure) were from Aldrich-Chemie (Steinheim, Germany). 1-Chloro-2-nitrobenzene and 4-chloro-3-nitrobenzoic acid were purchased from Fluka Chemie AG (Buchs, Switzerland). Chemical reagents and buffers were of the highest quality commercially available. Rat liver GST 4-4 was purified as described before (20).

**Syntheses.** Methyl 4-chloro-3-nitrobenzoate (**4b**) and *n*-butyl 4-chloro-3-nitrobenzoate (**5b**) were synthesized by esterification of 4-chloro-3-nitrobenzoic acid with the corresponding alcohols. In short, a mixture of 4 g (20 mmol) of 4-chloro-3-nitrobenzoic acid, 1.8 mL of sulfuric acid (95–98%), and 120 mL of methanol or *n*-butanol for **4b** and **5b**, respectively, was refluxed while stirring for 18 h. After the solution had cooled to room temperature, 75 mL of water was added. For purification of substrate **4b**, the methanol was evaporated and the residual water phase was neutralized with sodium bicarbonate, in which **4b** is insoluble. The crystals were filtered, washed with cold water, and dried. Recrystallization from methanol gave white crystals of **4b** in a yield of 96%, mp 80 °C. <sup>1</sup>H-NMR (<sup>2</sup>H-DMSO): δ 3.9 (s, CH<sub>3</sub>, 3H), 7.9 (d, H<sub>5</sub>,  $J_{56} = 8.0$  Hz, 1H), 8.2 (dd, H<sub>6</sub>,  $J_{56} = 8.0$  Hz,  $J_{26} = 1.33$  Hz, 1H), 8.5 (d, H<sub>2</sub>,  $J_{26} = 1.33$  Hz, 1H). For purification of **5b** the *n*-butanol was slowly evaporated. The residual water phase, which contained oily drops, was extracted with ethyl acetate, and subsequently the ethyl acetate fractions were washed with a 5% (w/v) sodium bicarbonate solution to remove unreacted 4-chloro-3-nitrobenzoic acid. The ethyl acetate was dried over sodium sulfate and evaporated in vacuo. The yellow oil (yield 45%) appeared to be pure as judged from NMR and HPLC [assay used for determination of extinction coefficient (20)]. <sup>1</sup>H-NMR (<sup>2</sup>H-DMSO): δ 0.9 (t, CH<sub>3</sub>,  $J = 6.67$  Hz, 3H), 1.42 (m, CH<sub>2</sub>, 2H), 1.70 (m, CH<sub>2</sub>, 2H), 4.3 (t, CH<sub>2</sub>,  $J = 6.67$  Hz, 2H), 7.9 (d, H<sub>5</sub>,  $J_{56} = 8.0$  Hz, 1H), 8.2 (dd, H<sub>6</sub>,  $J_{56} = 8.0$  Hz,  $J_{26} = 1.33$  Hz, 1H), 8.5 (d, H<sub>2</sub>,  $J_{26} = 1.33$  Hz, 1H).

*tert*-Butyl 4-chloro-3-nitrobenzoate (**6b**) was synthesized by adding 4 g (20 mmol) of 4-chloro-3-nitrobenzoic acid to 25 mL of dichloromethane and cooling this mixture to –20 °C in a flask able to resist 2 atm of pressure. With the aid of a CO<sub>2</sub>/acetone mixture 20 mL of isobutylene was condensed. The liquid isobutylene was subsequently added to the dichloromethane mixture via a calcium chloride tube. After addition of 0.2 mL of sulfuric acid (95–98%), the flask was closed and shaken for 2 days at room temperature. After the reaction mixture had been cooled, it was poured into 300 mL of a saturated sodium bicarbonate solution. This mixture was extracted three times with dichloromethane. The dichloromethane fractions were washed with a 5% (w/v) sodium bicarbonate solution, water, and a saturated sodium chloride solution, respectively. To remove polymers, the dichloromethane phase was eluted over a small silica column, dried over sodium sulfate, and finally the dichloromethane was evaporated. The residue was purified over a silica column, eluted with a mixture of petroleum ether (40/60) and ether (10:1). The yield of the white crystalline product was 3 g (58%), mp 68 °C. <sup>1</sup>H-NMR (<sup>2</sup>H-DMSO): δ 1.6 (s, CH<sub>3</sub>, 9H), 7.6 (d, H<sub>5</sub>,  $J_{56} = 10.0$  Hz, 1H), 8.1 (dd, H<sub>6</sub>,  $J_{56} = 10.0$  Hz,  $J_{26} = 3.34$  Hz, 1H), 8.4 (d, H<sub>2</sub>,  $J_{26} = 3.34$  Hz, 1H).

Synthesis of 1-bromo-4-chloro-3-nitrobenzene (**10b**) was accomplished according to Hammond and Modic (22). To a mixture of 1 g (6.35 mmol) of 1-chloro-2-nitrobenzene, 1 g of Ag<sub>2</sub>SO<sub>4</sub>, and 10 mL of sulfuric acid (95–98%) was slowly added 0.4 mL of bromine. This mixture was heated on a water bath of 80 °C for 5 h under constant stirring. After cooling, water was added to the reaction mixture and subsequently it was extracted with diethyl ether. The ether extract was dried over

**Table 1. R Groups in 2-Substituted 1-Chloro-4-nitrobenzenes (a-Compounds) and 4-Substituted 1-Chloro-2-nitrobenzenes (b-Compounds) and Their Reference Codes<sup>a</sup>**

R			$\lambda_{\max}$ (nm)		$\epsilon$ (mM <sup>-1</sup> cm <sup>-1</sup> )
			substrates b	GS-conjugates b	
NO <sub>2</sub>	<b>1a</b>	<b>1b</b>	250	340 <sup>b</sup>	9.6 <sup>b</sup>
CHO	<b>2a</b>	<b>2b</b>	245	304 <sup>c</sup>	10.0 <sup>c</sup>
COC <sub>6</sub> H <sub>5</sub>	<b>3a</b>	<b>3b</b>	260	306	14.1 ± 0.4
CO <sub>2</sub> CH <sub>3</sub>	<b>4a</b>	<b>4b</b>	232	370	3.4 ± 0.02
CO <sub>2</sub> (CH <sub>2</sub> ) <sub>3</sub> CH <sub>3</sub>	<b>5a</b>	<b>5b</b>	233	370	2.9 ± 0.1
CO <sub>2</sub> C(CH <sub>3</sub> ) <sub>3</sub>	<b>6a</b>	<b>6b</b>	232	289	16.4 ± 1.2
CN	<b>7a</b>				
CF <sub>3</sub>	<b>8a</b>	<b>8b</b>	253	365 <sup>c</sup>	2.2 <sup>c</sup>
Cl	<b>9a</b>	<b>9b</b>	221	383 <sup>d</sup>	0.7 <sup>d</sup>
Br	<b>10a</b>	<b>10b</b>	223	380	1.70 ± 0.01
CO <sub>2</sub> C <sub>6</sub> H <sub>5</sub>		<b>11b</b>	271	294	18.8 ± 4.5
CO <sub>2</sub> C <sub>6</sub> H <sub>4</sub> ( <i>t</i> Bu)		<b>12b</b>	230	282	<sup>e</sup>

<sup>a</sup> The maximal absorbance wavelength ( $\lambda_{\max}$ ) of the 4-substituted 1-chloro-2-nitrobenzenes and their corresponding GS-conjugates are shown, as well as the extinction coefficients ( $\epsilon$ ) of the GS-conjugates, which are determined at the  $\lambda_{\max}$  of the GS-conjugates [determined according to Van der Aar *et al.* (20)] and are the mean ± SD of at least three independent experiments. <sup>b</sup> Taken from Habig and Jakoby (43). <sup>c</sup> Taken from Chen *et al.* (41). <sup>d</sup> Taken from Keen *et al.* (40). <sup>e</sup> Not determined.

magnesium sulfate, and the diethyl ether was evaporated. Recrystallization of the solid residue from ethanol gave light yellow crystals in a yield of 29%, mp 69 °C. <sup>1</sup>H-NMR (<sup>2</sup>H-chloroform):  $\delta$  7.4 (d, H<sub>5</sub>,  $J_{56}$  = 8.0 Hz, 1H), 7.6 (dd, H<sub>6</sub>,  $J_{56}$  = 8.0 Hz,  $J_{26}$  = 0.67 Hz, 1H), 8.0 (d, H<sub>2</sub>,  $J_{26}$  = 0.67 Hz, 1H).

Phenyl 4-chloro-3-nitrobenzoate (**11b**) was synthesized by converting 4-chloro-3-nitrobenzoic acid to the corresponding benzoyl chloride, followed by a reaction with phenol. 4-Chloro-3-nitrobenzoic acid (1 g, 5 mmol) was mixed with 1 g (5 mmol) of phosphorus pentachloride and refluxed for 2 h at 80 °C under a nitrogen atmosphere. After cooling the reaction mixture, phosphorus oxychloride was removed by distillation under reduced pressure (25 °C/20 mmHg). The residual 4-chloro-3-nitrobenzoyl chloride was used without further purification. Phenol, 0.5 g (5 mmol), was dissolved in 5 mL of dry pyridine and added to the benzoyl chloride derivative. This reaction mixture was refluxed at 90 °C for 40 min. After the mixture had been cooled, it was poured into 20 mL of 2 M hydrochloric acid. The aqueous phase was decanted from the precipitated oil and stirred vigorously with 10 mL of a saturated sodium carbonate solution. The resulting solid material was filtered and washed with cold water. Recrystallization from ethanol gave yellow-orange crystals in a yield of 4%, mp 70 °C. <sup>1</sup>H-NMR (<sup>2</sup>H-DMSO):  $\delta$  7.4 (m, C<sub>6</sub>H<sub>5</sub>, 3H), 7.5 (m, C<sub>6</sub>H<sub>5</sub>, 2H), 8.1 (d, H<sub>5</sub>,  $J_{56}$  = 6.67 Hz, 1H), 8.4 (dd, H<sub>6</sub>,  $J_{56}$  = 6.67 Hz,  $J_{26}$  = 3.34 Hz, 1H), 8.7 (d, H<sub>2</sub>,  $J_{26}$  = 3.34 Hz, 1H).

3'-*tert*-Butylphenyl 4-chloro-3-nitrobenzoate (**12b**) was synthesized by reacting 4-chloro-3-nitrobenzoyl chloride with 3'-*tert*-butylphenol (as described for the synthesis of 4-chloro-3-nitrophenylbenzoate). After cooling the reaction mixture, 20 mL 2 M hydrochloric acid was added after which the pH was adjusted to 6–7 with a saturated sodium carbonate solution. This solution was extracted with diethyl ether and the collected diethyl ether fractions were washed five times with 2 M sodium hydroxide to remove unreacted 3'-*tert*-butylphenol. The diethyl ether fraction was dried over magnesium sulfate and evaporated in vacuo. 3'-*tert*-Butylphenyl 4-chloro-3-nitrobenzoate was obtained as a light yellow oil in a yield of 5%. <sup>1</sup>H-NMR (<sup>2</sup>H-DMSO):  $\delta$  1.4 (s, CH<sub>3</sub>, 9H), 7.1–7.5 (m, C<sub>6</sub>H<sub>4</sub>, 4H), 8.1 (d, H<sub>5</sub>,  $J_{56}$  = 8.0 Hz, 1H), 8.4 (dd, H<sub>6</sub>,  $J_{56}$  = 8.0 Hz,  $J_{26}$  = 2.0 Hz, 1H), 8.8 (d, H<sub>2</sub>,  $J_{26}$  = 2.0 Hz, 1H).

**Kinetic Parameters.** The determination of the enzyme kinetic parameters  $K_m$ ,  $k_{\text{cat}}$ , and  $k_{\text{cat}}/K_m$  for the GST 4-4-catalyzed GSH conjugation of 2-substituted 1-chloro-4-nitrobenzenes (**a**-compounds, Table 1) and the rate constants ( $k_s$ ) of the corresponding base-catalyzed reactions has been described in previous studies (20, 21). The same kinetic parameters were

determined for the GSH conjugation of 4-substituted 1-chloro-2-nitrobenzenes (**b**-compounds, Table 1) when catalyzed by base and GST 4-4. In short, the formation of GS-conjugates was followed spectrophotometrically with time at the maximal absorbance wavelength ( $\lambda_{\max}$ ) of the GS-conjugates (Table 1). For all examined substrates no appreciable absorbance of reactants was observed at the wavelengths that were used to monitor the formation of GS-conjugates. The extinction coefficients ( $\epsilon$ ) of the GS-conjugates were determined at the wavelengths that were used to follow the reactions according to Van der Aar *et al.* (20) and are shown in Table 1. The assay medium for determination of GST-catalyzed conjugation rates contained 0.1 M potassium phosphate buffer (pH 6.5, 0.1 mM EDTA), GST 4-4 (different concentrations depending on substrate tested), 1 mM GSH, and various concentrations of substrate. The incubations were performed at 37 °C. The base-catalyzed GSH conjugation reaction was performed in 0.1 M potassium phosphate buffer (pH 9.2, 0.1 mM EDTA), at 50 °C with a GSH concentration of 10 mM. Under these experimental conditions no GSH was oxidized, as determined with 2,2'-dinitro-5,5'-dithiodibenzoic acid.

**Computational Methods and Molecular Modeling.** The minimal energy conformers of the compounds were calculated, and it was assumed that these minimal energy conformers were those that would bind to the enzyme. This might, however, not be the actual situation. The initial conformations of the 4-substituted 1-chloro-2-nitrobenzenes (Table 1, **1b**–**12b**) were generated from the geometry-optimized conformation (15) of 1-chloro-2,4-dinitrobenzene (CDNB, **1a,b**) using the molecular modeling package ChemX (23). Macromodel (24) was used for molecular mechanics conformational analyses on the generated compounds. If necessary, a large number of conformations was generated by changing all rotatable bonds with increments of 30° (compounds **5b**, **6b**, **11b**, and **12b**). Generally, the conformations were energy minimized with the Amber force field (25, 26), using Batchmin (27). For the ketone- and ester-substituted substrates several low-energy conformations were generated with different orientations of the carbonyl oxygen atom (see Figure 2).

The quantum chemical program package GAMESS-UK (28, 29) was used for the *ab initio* calculations described. The geometries of the lowest energy conformations for all substrates obtained with Macromodel, were *ab initio* optimized at the RHF (restricted Hartree–Fock) level using the STO-3G (Slater type orbital composed of 3 Gaussians) (30) minimal basis set. On the resulting STO-3G geometries, a single-point energy calculation and a DMA (distributed multipole analysis) calculation (31)

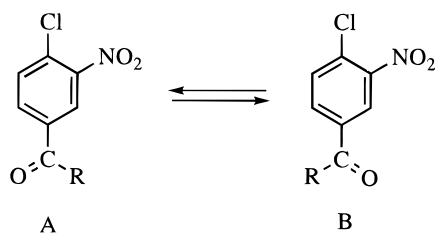


**Figure 2.** Low-energy conformations of 1-chloro-2-nitrobenzenes with ketone or ester substituents on the 4-position.

were performed using the RHF method in an SV (split valence) 6-31G (32, 33) basis set. Charge distributions and energy values ( $E_{\text{homo}}$  and  $E_{\text{lumo}}$ ) of the lowest total energy conformation of the ketone- and ester-substituted substrates were used in the SAR analyses (energy difference between various conformations < 4 kJ/mol).

The molecular modeling program ChemX (23) was used for the rigid fitting procedure in which compounds are fitted allowing only global rotations and translations. All 4-substituted 1-chloro-2-nitrobenzenes (**1b–12b**) were fitted onto the diequatorial conformation of benzo[*a*]pyrene 7(*R*),8(*S*)-dial 9(*S*),10(*R*)-epoxide (BPDE) with the rigid fitting procedure (23). The sites of GSH attack in the different substrates were matched onto each other. Furthermore, one of the oxygen atoms of the nitro group at the 2-position of the substrates was fitted onto the oxygen atom of the 8-hydroxyl group of BPDE. If the distance between fitted atoms was less than 0.25 Å, the fitted conformation was accepted. The energy of the fitted conformation was calculated with *ab initio* methods [RHF/SV 6-31G (32, 33)]. If the energy difference between the minimal energy conformation and the fitted conformation was less than 21 kJ/mol, the fitted conformation was accepted and a DMA (31) was carried out.

**Structure–Activity Relationships.** Single- and multiple-regression analyses were performed for determination of correlations between kinetic parameters of the GST 4-4-catalyzed ( $K_m$ ,  $k_{\text{cat}}$ , and  $k_{\text{cat}}/K_m$ ) and the base-catalyzed ( $k_s$ ) GSH conjugation reaction of 4-substituted 1-chloro-2-nitrobenzenes (**1b–12b**) with eight physicochemical parameters and five computer-calculated parameters. These correlations were compared with those for the 2-substituted 1-chloro-4-nitrobenzenes (**1a–10a**) previously determined (21).

To probe the steric effects of the substituents, the multidimensional Sterimol parameters ( $L$ ,  $B_1$ , and  $B_5$ ) were used (34). The hydrophobic fragment constant  $f$  of Rekker (35) was used to probe lipophilicity effects of the substituents. The Hammett  $\sigma_p$  constants were used as electronic parameters (taken from ref 36). Despite the steric influences in the *ortho* substituents, the  $\sigma$  values for *para* substituents ( $\sigma_p$ ) approximate those for the *ortho* substituents in the case of 2-substituted 1-chloro-4-nitrobenzenes (21). When substituents are directly conjugated with the reaction center, “through resonance” may occur. Such interactions may either facilitate or hinder attainment of the transition state. Therefore, an alternative Hammett constant,  $\sigma^-$ , has been defined in order to correct for “through resonance” (37). Furthermore, two additional electronic parameters were defined (38) to separate the inductive component of substituents (field effect,  $\mathcal{F}$ ) from the resonance component ( $\mathcal{R}$ ) (taken from ref 36). The physicochemical parameters actually used in the SAR analyses are shown in Table 3.

To obtain the computer-calculated molecular parameters of the substrates (**1b–12b**), the lowest energy conformations of the substrates were subjected to energy and charge distribution calculations, leading to  $E_{\text{homo}}$  and  $E_{\text{lumo}}$ , to charges on the attacked C-atom ( $C_1$ ), and to charges on the *ortho* and *para* substituents, respectively. For the ten 2-substituted 1-chloro-4-nitrobenzenes (**1a–10a**) these parameters were calculated and tabulated in a previous study (21), while the molecular parameters of the 4-substituted 1-chloro-2-nitrobenzenes were calculated in this study and are shown in Table 3.

Only correlations with a Student's *t* test's *t* value of  $>|2|$  were considered to be significant. In case of multiple regression the

**Table 2.** Kinetic Parameters of the GST 4-4-Catalyzed ( $K_m$ ,  $k_{\text{cat}}$ ,  $k_{\text{cat}}/K_m$ ) and the Base-Catalyzed ( $k_s$ ) GSH Conjugation of 4-Substituted 1-Chloro-2-nitrobenzenes (**b-Compounds**)

substrate	$k_s$ ( $\times 10^{-4}$ $\mu\text{M}^{-1} \text{min}^{-1}$ )	$K_m$ ( $\mu\text{M}$ )	$k_{\text{cat}}$ ( $\text{min}^{-1}$ )	$k_{\text{cat}}/K_m$ ( $\times 10^{-2} \mu\text{M}^{-1}$ $\text{min}^{-1}$ )
<b>1b</b>	420 ± 20	156 ± 36	137 ± 14	93 ± 19
<b>2b</b>	23 ± 1	73 ± 6	31 ± 9	35 ± 8
<b>3b</b>	32 ± 1	41 ± 5	6.5 ± 1.0	21 ± 4
<b>4b</b>	7.0 ± 0.7	308 ± 57	8.5 ± 0.7	2.7 ± 0.8
<b>5b</b>	10.7 ± 1.2	50 ± 5	1.70 ± 0.01	3.4 ± 0.3
<b>6b</b>	2.8 ± 0.4	<i>a</i>	<i>a</i>	<i>a</i>
<b>8b</b>	5.3 ± 0.3	748 ± 180	7.3 ± 2.0	0.7 ± 0.1
<b>9b</b>	<i>b</i>	<i>b</i>	<i>b</i>	<i>b</i>
<b>10b</b>	<i>b</i>	<i>b</i>	<i>b</i>	<i>b</i>
<b>11b</b>	40.2 ± 3.8	46 ± 13	6.8 ± 1.5	15 ± 2
<b>12b</b>	<i>c</i>	<i>d</i>	<i>d</i>	<i>d</i>

<sup>a</sup> No detectable GSH conjugation up to 300  $\mu\text{M}$  of substrate **6b** ( $k_{\text{cat}} < 0.06 \text{ min}^{-1}$  using 250  $\mu\text{g/mL}$  of GST 4-4). <sup>b</sup> No detectable GSH conjugation up to 1000  $\mu\text{M}$  of substrates **9b** and **10b** ( $k_{\text{cat}} < 1.5$  and  $0.6 \text{ min}^{-1}$ , respectively using 250  $\mu\text{g/mL}$  of GST 4-4). <sup>c</sup> GSH conjugation observed but not quantified (no extinction coefficient determined). <sup>d</sup> No detectable GSH conjugation up to 300  $\mu\text{M}$  of substrate **12b** (no  $k_{\text{cat}}$  limit calculated due to the unavailability of the extinction coefficient).

intercorrelation between the two independent parameters was checked ( $r < 0.5$ ).

## Results and Discussion

In the present study eleven 4-substituted 1-chloro-2-nitrobenzenes (compounds **1b–12b**, Table 1) were analyzed for their capacity to conjugate to GSH when catalyzed by GST 4-4 or base. When possible, the corresponding kinetic parameters ( $K_m$ ,  $k_{\text{cat}}$ ,  $k_{\text{cat}}/K_m$ , and  $k_s$ , respectively) of these compounds were determined and compared (Table 2). SAR analyses were performed by correlating the kinetic parameters for the GSH conjugation of 4-substituted 1-chloro-2-nitrobenzenes with eight physicochemical parameters ( $\sigma_p$ ,  $\sigma_p^-$ ,  $\mathcal{F}$ ,  $\mathcal{R}$ ,  $L$ ,  $B_1$ ,  $B_5$ , and  $f$ ) and with five computer-calculated molecular parameters of the substrates ( $E_{\text{lumo}}$ ,  $E_{\text{homo}}$ , and the charges on  $C_1$  and on the *ortho* and *para* substituents) (Table 3). Correlations were only considered to be significant when  $t > |2|$ . These SAR's are compared with the previously obtained SAR's for the base- and GST 4-4-catalyzed GSH conjugation of ten 2-substituted 1-chloro-4-nitrobenzenes (compounds **1a–10a**, Table 1) (21).

Furthermore, eight 4-substituted 1-chloro-2-nitrobenzenes and three 2-substituted 1-chloro-4-nitrobenzenes are used to extend the previously described substrate model for rat GST 4-4, which was obtained by molecular modeling techniques and which was among others based on some 2-substituted 1-chloro-4-nitrobenzenes (**1a–5a**, **9a**, and **10a**) (Figure 1) (15).

**Apparent Michaelis Constant ( $K_m$ ).** The experimentally determined apparent  $K_m$  values of 4-substituted 1-chloro-2-nitrobenzenes for GST 4-4 are shown in Table 2. The lowest  $K_m$  values, suggestive of a high apparent affinity, were found for substrates with a phenyl substituent (**3b** and **11b**). The highest  $K_m$  value by far was found for the  $\text{CF}_3$ -substituted substrate **8b**. For the *p*-Cl- and *p*-Br-substituted compounds (**9b** and **10b**), no detectable GST 4-4-catalyzed GSH conjugation was observed up to 1 mM (Table 2,  $k_{\text{cat}} < 1.5$  and  $0.6 \text{ min}^{-1}$ , respectively, when using 250  $\mu\text{g/mL}$  of GST 4-4). On the basis of the higher GSH conjugation rates of most 4-substituted 1-chloro-2-nitrobenzenes when compared to the

**Table 3. Computer-Calculated Molecular Parameters<sup>a</sup> of 4-Substituted 1-Chloro-2-nitrobenzenes Examined in This Study and the Physicochemical Parameters of the Substituents Actually Used in This Study**

substrates	$\sigma_p^-$	$L$	$B_5$	$f$	charge <sup>b</sup>			$E_{\text{lumo}}^c$ (kJ/mol)	$E_{\text{homo}}^c$ (kJ/mol)
					attacked C atom	<i>o</i> -nitro substituent	<i>para</i> substituent		
<b>1b</b>	1.27	3.44	2.44	-0.039	0.265	-0.148	-0.169	44.3	-1094.4
<b>2b</b>	1.02	3.53	2.36	-0.333	0.179	-0.171	0.142	17.5	-1027.5
<b>3b</b>	0.87	4.57 <sup>e</sup>	5.98 <sup>e</sup>	0.926	0.173	-0.179	0.188	36.5	-946.3
<b>4b</b>	0.76	4.73	3.36	0.181	0.184	-0.172	0.080	37.0	-1021.6
<b>5b</b>	0.76	8.00	5.85	1.738	0.183	-0.172	0.086	39.4	-1017.6
<b>6b</b>	<i>d</i>	<i>d</i>	<i>d</i>	1.738	0.182	-0.173	0.097	42.1	-1013.8
<b>8b</b>	0.71	3.30	2.61	1.223	0.185	-0.148	0.093	-8.5	-1060.4
<b>9b</b>	0.21	3.52	1.80	0.933	0.168	-0.177	-0.147	26.0	-996.3
<b>10b</b>	0.23	3.82	1.95	1.134	0.148	-0.180	-0.008	37.1	-959.7
<b>11b</b>	0.76	8.13	3.50	1.590	0.185	-0.169	0.079	32.3	-913.8

<sup>a</sup> The computer-calculated parameters were taken from the conformation with the lowest total energy. <sup>b</sup> Charges were obtained from DMA calculations. <sup>c</sup> Energy values were obtained from SV 6-31G calculations. <sup>d</sup> This physicochemical parameter was not available for a *tert*-butyl ester substituent. <sup>e</sup> Phenyl ring is twisted out of the aromatic plane (90°).

2-substituted 1-chloro-4-nitrobenzenes (discussed later), it was expected that **9b** and **10b** would also be conjugated to GSH. Unfortunately, however, the extinction coefficients of the corresponding GS-conjugates of **9b** and **10b** are low (0.7 and 1.7 mM<sup>-1</sup> cm<sup>-1</sup>, Table 1), thereby prohibiting a sensitive and accurate measurement. Instead, in an incubation mixture of GST 4-4 and GSH, the decrease in substrates **9b** and **10b** was checked with time by HPLC with UV detection at  $\lambda_{\text{max}}$  of the substrates. After 30 min, a measurable decrease in concentrations of substrates was observed ( $\pm 8\%$ ) when compared to the control incubations in which no GSH was present, indicating that some GSH conjugation may have taken place (data not shown). Detectable GSH conjugation was not observed for substrates **6b** and **12b** up to 300  $\mu\text{M}$ . This could also be a result of the limited solubility of these substrates or to steric restrictions in this area of the active site of GST 4-4. Electronic restrictions probably play no role because measurable GSH conjugation of **6b** and **12b** was observed when catalyzed by base (Table 2).

Single- and multiple-regression analyses between the  $K_m$  values of GST 4-4 for the GSH conjugation of 4-substituted 1-chloro-2-nitrobenzenes (compounds **1b**–**12b**) (Table 2) with all eight physicochemical and five computer-calculated parameters discussed before, showed no statistically significant correlations ( $t < |2|$ ) or correlations with a low correlation coefficient ( $r < 0.7$ ). Previously, significant correlations were neither found for the  $K_m$  values of 2-substituted 1-chloro-4-nitrobenzenes (**1a**–**10a**) with the above mentioned parameters (21). Apparently, the affinity of the examined substrates (**1a**–**10a** and **1b**–**12b**) toward GST 4-4 (i.e., formation of enzyme–substrate complexes) is not solely dependent on any of these molecular parameters.

Recently, Rietjens *et al.* found a linear correlation between the  $K_m$  values for the GSH conjugation of five fluoronitrobenzenes catalyzed by rat liver cytosol and log  $P_{\text{octanol}}$  ( $r = -0.997$ ) (18). In a successive study individual GSTs of rat (1-1 and 3-3) and man (A1-1 and M1a-1a) were subjected to similar regression analyses with four fluoronitrobenzenes with varying numbers of F atoms (19). For rat GST 1-1, a linear correlation was found between the  $K_m$  and log  $P_{\text{octanol}}$  ( $r = -0.989$ ), while for rat GST 3-3 this correlation was less significant ( $r = -0.874$ ), indicating that correlations between  $K_m$  and log  $P$  depend on the individual GSTs. The fact that no such correlations were found in the present study could well be due to the inclusion of structurally more different

substituents, giving rise to additional steric and electronic effects.

A qualitative comparison of the apparent  $K_m$  values of GST 4-4 for the 4-substituted 1-chloro-2-nitrobenzenes and the previously determined  $K_m$  values for the 2-substituted series of 1-chloro-4-nitrobenzenes (20) shows that there are significant differences. Substrates with bulky substituents at the *para* position have a lower apparent  $K_m$ . Substrate **3b**, for example, has an almost four times lower  $K_m$  than substrate **3a** (41 and 154  $\mu\text{M}$ , respectively). From the calculated minimal energy conformation it appeared that in both **3a** and **3b**, the phenyl ring of the benzophenone substituent is twisted out of the aromatic plane, due to intramolecular steric hindrance. The difference in  $K_m$  values of **3a** and **3b** could well be due to this difference in orientation of the benzophenone phenyl rings relative to the aromatic plane. The *para* substituent in **3b** could also provide additional lipophilic and/or electronic interactions with amino acids in the active site of the GST 4-4 protein, which are absent in the case of a NO<sub>2</sub> substituent in **3a**. The *para*-phenyl ester-substituted substrate (**11b**) also showed a low  $K_m$  value (46  $\mu\text{M}$ ), again suggesting that there are additional lipophilic and/or electronic interactions between the phenyl ring and GST 4-4. Substrate **5b** (*n*-butyl ester) has a  $K_m$  almost seven times lower than substrate **5a** (50 and 341  $\mu\text{M}$ , respectively). Steric restrictions in the active site in accommodating the *ortho*-substituted *n*-butyl ester of **5a** are probably not the reason for this, because the corresponding methyl ester derivative (**4a**) has an even higher  $K_m$  (554  $\mu\text{M}$ ). The high affinity of **5b** for GST 4-4 is therefore more likely explained by lipophilic interactions with the protein. The *para*-substituted methyl ester derivative (**4b**) has a six times higher  $K_m$ , and thus a lower affinity than the corresponding *para* *n*-butyl ester derivative (**5b**), probably because a methyl group provides less lipophilicity than the flexible *n*-butyl chain in **5b** (Table 2).

**Turnover Number  $k_{\text{cat}}$ .** Of the 4-substituted 1-chloro-2-nitrobenzenes, the NO<sub>2</sub>- and CHO-substituted compounds (**1b** and **2b**) result in the highest and second highest  $k_{\text{cat}}$  values (Table 2). A comparison of the  $k_{\text{cat}}$  values of the 2-substituted 1-chloro-4-nitrobenzenes (**1a**–**10a**) (20) and the 4-substituted 1-chloro-2-nitrobenzenes (**1b**–**12b**) (Figure 3) shows that substrates **2b**–**4b** have higher  $k_{\text{cat}}$  values than their *ortho*-substituted analogues, albeit to different extents. The *n*-butyl ester substrate **5a** has a  $k_{\text{cat}}$  seven times higher than **5b** ( $12.1 \pm 0.8$  and  $1.70 \pm 0.01 \text{ min}^{-1}$ , respectively), and the *o*- and *p*-CF<sub>3</sub>-

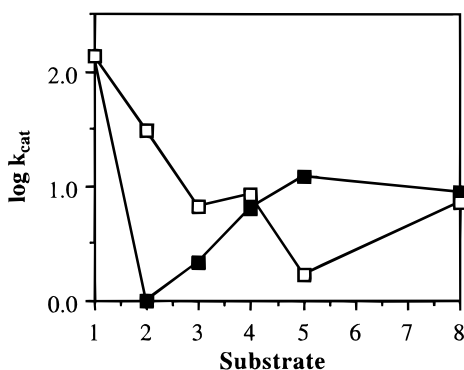


**Figure 3.** Comparison of  $k_{\text{cat}}$  values for the GST 4-4-catalyzed GSH conjugation of 2-substituted 1-chloro-4-nitrobenzenes (**a**-compounds, ■) and 4-substituted 1-chloro-2-nitrobenzenes (**b**-compounds, □).

substituted substrates **8a** and **8b** have almost identical  $k_{\text{cat}}$  values ( $\pm 8 \text{ min}^{-1}$ ).

All substrates under investigation will be conjugated to GSH via a nucleophilic aromatic substitution ( $S_{\text{N}}\text{Ar}$ ) mechanism. The rate-determining step in this type of reactions is the formation of a Meisenheimer intermediate, in which both the nucleophile ( $\text{GS}^-$ ) and the leaving group ( $\text{Cl}^-$ ) are bound to the substrate and in which a net charge of  $-1$  is distributed over the intermediate (39). Electron-withdrawing substituents *ortho* and/or *para* relative to the reaction center will stabilize this net negative charge in the Meisenheimer intermediates.

Single-regression analyses between  $\log k_{\text{cat}}$  of GST 4-4 for the GSH conjugation of 2-substituted 1-chloro-4-nitrobenzenes and  $\sigma_{\text{p}}^-$ , the Hammett electronic constant corrected for "through resonance", showed no significant correlation for the 2-substituted analogues ( $t < 2$ ), while the 4-substituted analogues did:

$$\log k_{\text{cat}} = 2.77(\pm 0.67)\sigma_{\text{p}}^- - 1.41(\pm 0.61) \quad (1)$$

$$r = 0.901 \quad s = 0.319 \quad n = 6$$

The latter equation indicates that the higher the electron-withdrawing capacity of the substituents becomes ( $\sigma_{\text{p}}^-$  increases), the more efficient the Meisenheimer intermediates are stabilized and the higher the  $k_{\text{cat}}$  values become. Within the present series of substituents,  $\text{NO}_2$  has the highest  $\sigma_{\text{p}}^-$ , and thus the highest  $k_{\text{cat}}$  value is observed for substrate **1b**. From an electronic point of view the 4-substituted 1-chloro-2-nitrobenzenes should have a higher GSH conjugation rate than the 2-substituted 1-chloro-4-nitrobenzenes. The *para*-substituted analogues will have a more efficient stabilization of the negative charge in the Meisenheimer complexes because the *ortho*  $\text{NO}_2$  substituent is closest to the reaction center. Exceptions to this general statement are possibly due to extra steric and lipophilic interactions between the *ortho* and/or *para* substituents and amino acids in the active site. The fact that  $k_{\text{cat}}$  for the 2-substituted 1-chloro-4-nitrobenzenes (**1a–10a**) did not correlate with  $\sigma_{\text{p}}^-$  indicates that "through resonance" on the *ortho* position is not taking place, probably because of steric hindrance in the Meisenheimer intermediates between the *ortho* substituent and the Cl atom at  $\text{C}_1$ , while in the 4-substituted analogues (**1b–12b**) this steric hindrance apparently plays no significant role.

A relatively high correlation coefficient was found when the  $k_{\text{cat}}$  of GST 4-4 for the GSH conjugation of 2-substi-

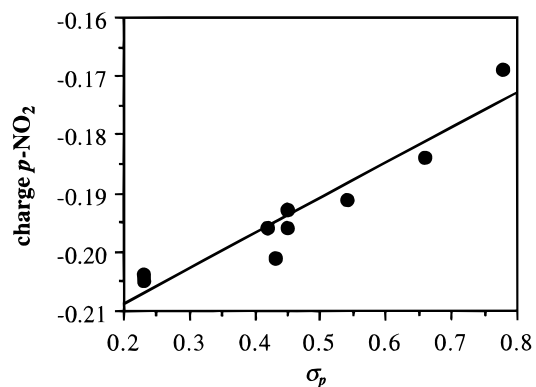


**Figure 4.** Correlation between  $\sigma_{\text{p}}$  values of the 2-substituents and the calculated charge on  $p\text{-NO}_2$  of 2-substituted 1-chloro-4-nitrobenzenes (**1a–10a**). The corresponding equation is as follows: ( $\text{charge } p\text{-NO}_2$ ) =  $0.060(\pm 0.007)\sigma_{\text{p}} - 0.221(\pm 0.003)$ ,  $r = 0.952$ ,  $s = 0.003$ ,  $n = 10$ .

tuted 1-chloro-4-nitrobenzenes (**1a–10a**) was correlated with the calculated charge on the  $p\text{-NO}_2$  substituents of the substrates:

$$\log k_{\text{cat}} = 41.8(\pm 7.2)(\text{charge } p\text{-NO}_2) + 9.1(\pm 1.4) \quad (2)$$

$$r = 0.922 \quad s = 0.226 \quad n = 8$$

The CHO-substituted substrate (**2a**) was excluded from eq 2 because it appeared to be an outlier according to statistical rules. Equation 2 implies that when the negative charge on  $p\text{-NO}_2$  increases, the  $k_{\text{cat}}$  increases. The amount of negative charge on  $p\text{-NO}_2$  indirectly reflects the electron-withdrawing capacity of the *ortho* substituent ( $\sigma_{\text{o}}$ ). This is illustrated in Figure 4, in which the relation between  $\sigma_{\text{p}}$  of the 2-substituents and the calculated negative charges on the  $p\text{-NO}_2$  substituent in 2-substituted 1-chloro-4-nitrobenzenes is shown. With the corresponding equation (see legend to Figure 4) and known  $\sigma_{\text{p}}$  values, it is possible to predict the charge on the  $p\text{-NO}_2$  substituent and thus  $\sigma_{\text{o}}$ . When a regression was applied between  $k_{\text{cat}}$  and the charge on the *o*- $\text{NO}_2$  substituent in 4-substituted 1-chloro-2-nitrobenzenes (**1b–12b**), in contrast, no statistically significant correlation was found ( $t = 1.9$ ). Apparently, the charge on *o*- $\text{NO}_2$  is not an appropriate parameter to describe the electron-withdrawing capacity of the *para* substituents, probably by the lack of "through resonance" on the *o*- $\text{NO}_2$  substituent due to steric hindrance.

Multiple-regression analyses (although with a limited number of data points) with  $k_{\text{cat}}$  of the 4-substituted 1-chloro-2-nitrobenzenes (**1b–12b**) and  $\sigma_{\text{p}}^-$  and the Sterimol parameters  $L$  or  $B_5$  simultaneously revealed higher correlation coefficients than with the individual parameters ( $r = 0.90$  for  $\sigma_{\text{p}}^-$ ,  $0.74$  for  $L$ , and  $0.72$  for  $B_5$ ):

$$\log k_{\text{cat}} =$$

$$-0.16(\pm 0.05)L + 2.21(\pm 0.37)\sigma_{\text{p}}^- - 0.17(\pm 0.47) \quad (3)$$

$$r = 0.982 \quad s = 0.161 \quad n = 6$$

$$\log k_{\text{cat}} =$$

$$-0.16(\pm 0.05)B_5 + 2.23(\pm 0.38)\sigma_{\text{p}}^- - 0.31(\pm 0.45) \quad (4)$$

$$r = 0.981 \quad s = 0.165 \quad n = 6$$

These equations support our suggestion that, in addition to the electron-withdrawing capacity of the substituents and the possibility for "through resonance", also

steric factors play a role in the GST 4-4-catalyzed GSH conjugation of 4-substituted 1-chloro-2-nitrobenzenes. In the Sterimol system,  $L$  is defined as the length of the substituent along the axis of the bond between the first atom of the substituent and the parent molecule and  $B_5$  is the maximal width (34). Apparently, the  $L$  and  $B_5$  dimensions of the 4-substituents are limited and if these dimensions are exceeded, no GSH conjugation is possible anymore. This is probably the case for compound **12b**, which is conjugated to GSH when catalyzed by base but not by GST 4-4. Compared to the GST 4-4 substrate **11b**, **12b** has an identical  $L$  value but a much larger  $B_5$  value, thus preventing GSH conjugation.

Significant correlations were also found between  $\log k_{\text{cat}}$  of GST 4-4 for the GSH conjugation of 4-substituted 1-chloro-2-nitrobenzenes (**1b–12b**) and the hydrophobic fragment constant  $f$  of Rekker (35) ( $r = 0.828$ ) and the calculated charge on the reaction center,  $C_1$  ( $r = 0.769$ ). Multiple-regression analyses with both independent parameters, however, showed a higher correlation coefficient:

$$\log k_{\text{cat}} = 10.09(\pm 3.13)(\text{charge } C_1) - 0.51(\pm 0.14)f - 0.57(\pm 0.65) \quad (5)$$

$$r = 0.964 \quad s = 0.225 \quad n = 6$$

Although the regression analysis was performed with a limited number of data points, there is a trend that the lipophilicity of the *para* substituents is of importance in the height of the value of  $k_{\text{cat}}$ . The lipophilic properties of the *para* substituents should not be too high, because this seems to have a negative influence on  $k_{\text{cat}}$ . This statement is confirmed by the observation that the *para*-substituted *n*-butyl ester analogue (**5b**), with the highest  $f$  value, has the lowest  $k_{\text{cat}}$  within the 4-substituted 1-chloro-2-nitrobenzenes. The correlation with the charge on  $C_1$  is directly a result of the electron-withdrawing capacity of the 4-substituents: the higher this becomes, the higher the positive charge on  $C_1$  becomes, and thus, the higher the  $k_{\text{cat}}$ . Regression analysis between the  $k_{\text{cat}}$  values of the 2-substituted 1-chloro-4-nitrobenzenes (**1a–10a**) and  $f$  gave an equation which was not significant ( $t = -0.25$ ), indicating that lipophilicity of the *ortho* substituents is not important for GSH conjugation by GST 4-4.

**Specificity Constants  $k_{\text{cat}}/K_m$  and  $k_s$  Values.** The  $k_{\text{cat}}/K_m$  parameter (specificity constant) for enzymes comprises the processes of substrate binding, intermediate stabilization and release of products from the active site. In addition to substrates **1b** and **2b** of the 4-substituted 1-chloro-2-nitrobenzenes, substrates with *para* phenyl substituents (**3b** and **11b**) also show substantial GSH conjugation when catalyzed by base and by GST 4-4 (Table 2). Of both the 2-substituted 1-chloro-4-nitrobenzenes (**1a–10a**) and the 4-substituted 1-chloro-2-nitrobenzenes (**1b–12b**), substrate **1a,b** (CDNB) has the highest  $k_s$  and  $k_{\text{cat}}/K_m$  values (Table 2) due to the high electron-withdrawing capacity of the *o*- and *p*-NO<sub>2</sub> substituents resulting in the best stabilization of the Meisenheimer intermediate in the present series of compounds.

In Figure 5 it is shown that all 4-substituted 1-chloro-2-nitrobenzenes have higher  $k_s$  values than the 2-substituted 1-chloro-4-nitrobenzenes, except for the *tert*-butyl ester-substituted substrates **6a** and **6b**, which have identical  $k_s$  values. An overall comparison of  $k_{\text{cat}}/K_m$  values of the GSH conjugation of 2-substituted 1-chloro-

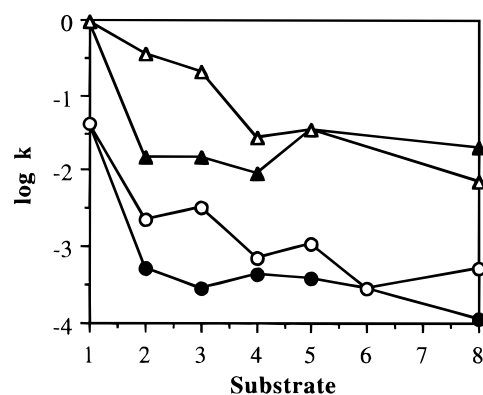


**Figure 5.** Comparison of  $k_s$  values for the base-catalyzed GSH conjugation of 2-substituted 1-chloro-4-nitrobenzenes (●) and 4-substituted 1-chloro-2-nitrobenzenes (○) and of  $k_{\text{cat}}/K_m$  values for the GST 4-4-catalyzed GSH conjugation of 2-substituted 1-chloro-4-nitrobenzenes (▲) and 4-substituted 1-chloro-2-nitrobenzenes (△).

4-nitrobenzenes and 4-substituted 1-chloro-2-nitrobenzenes (Figure 5) shows higher  $k_{\text{cat}}/K_m$  values for the latter series of substrates, except for the *n*-butyl ester analogues (**5a** and **5b**), which have identical values, and for the CF<sub>3</sub>-substituted substrates (**8a** and **8b**), from which the *ortho* analogue has the most efficient GSH conjugation. As discussed before, in the 4-substituted 1-chloro-2-nitrobenzenes (**1b–12b**), the NO<sub>2</sub>-substituent, with the highest electron-withdrawing capacity, is positioned *ortho* relative to the GSH conjugation site ( $C_1$ ) and thereby is closest to the reaction center, leading to an increased rate of conjugation compared to the corresponding 2-substituted 1-chloro-4-nitrobenzenes (**1a–10a**), in which the NO<sub>2</sub>-substituent is located *para* relative to  $C_1$ .

The Hammett  $\sigma_p^-$  constant, corrected for "through resonance" ( $\sigma_p^-$ ), was also used in regression analyses with the kinetic parameters  $k_s$  and  $k_{\text{cat}}/K_m$ . For the GSH conjugation of 2-substituted 1-chloro-4-nitrobenzenes (**1a–10a**), significant equations ( $t > |2|$ ) were obtained between  $k_s$  and  $\sigma_p^-$  and between  $k_{\text{cat}}/K_m$  and  $\sigma_p^-$ , but with low correlation coefficients (approximately 0.75). The corresponding regression analyses for the 4-substituted 1-chloro-2-nitrobenzenes (**1b–12b**), however, gave equations with high correlation coefficients:

$$\log k_s = 3.09(\pm 0.50)\sigma_p^- - 5.43(\pm 0.46) \quad (6)$$

$$r = 0.952 \quad s = 0.238 \quad n = 6$$

$$\log k_{\text{cat}}/K_m = 3.42(\pm 0.76)\sigma_p^- - 4.13(\pm 0.70) \quad (7)$$

$$r = 0.913 \quad s = 0.365 \quad n = 6$$

As was observed for  $k_{\text{cat}}$ , the process of "through resonance" is obviously of more importance in the GSH conjugation of 4-substituted 1-chloro-2-nitrobenzenes than of 2-substituted 1-chloro-4-nitrobenzenes, because of steric hindrance in the Meisenheimer intermediates between the *ortho* substituent and the Cl atom at  $C_1$ .

The slopes in the Hammett eqs 6 and 7 represent the  $\rho$  values, which give an indication of the sensitivity of the reaction for the electronic effects of the substituents. Upon regression analysis between  $\sigma_p^-$  and  $k_s$  for the base-catalyzed GSH conjugation of 4-substituted 1-chloro-2-nitrobenzenes, Keen *et al.* found a  $\rho$  value of 3.1 when using the substituents Cl, SO<sub>3</sub><sup>-</sup>, CONH<sub>2</sub>, COCH<sub>3</sub>, CHO, and NO<sub>2</sub> (40), and Chen *et al.* found a  $\rho$  value of 3.4 ± 0.2 when using the substituents SO<sub>3</sub><sup>-</sup>, SO<sub>2</sub>CH<sub>3</sub>, COCH<sub>3</sub>,

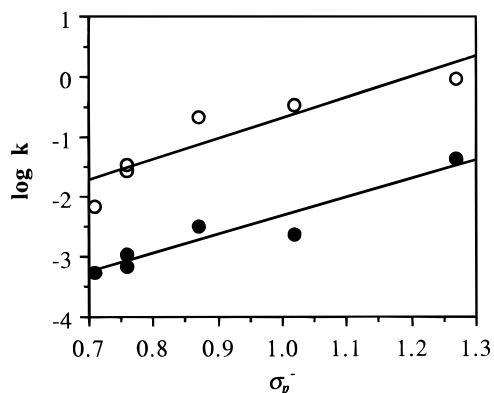


**Figure 6.** Kinetic constants of the base-catalyzed ( $k_s$ , ●) and the GST 4-4-catalyzed ( $k_{cat}/K_m$ , ○) GSH conjugation of 4-substituted 1-chloro-2-nitrobenzenes vs  $\sigma_p^-$ . Plots are based on eqs 6 and 7.

CHO, CF<sub>3</sub>, and NO<sub>2</sub> (41). These values correspond well to the  $\rho$  value found in the present study:  $3.09 \pm 0.50$  (eq 6). For the GST 4-4-catalyzed GSH conjugation of 4-substituted 1-chloro-2-nitrobenzenes, Chen *et al.* found a  $\rho$  value of  $2.4 \pm 0.6$  (41), which does neither differ significantly from the  $\rho$  value of  $3.4 \pm 0.8$  found in the present study (eq 7). When eqs 6 and 7 are transformed to Hammett plots (Figure 6), it can also be seen that the base-catalyzed as well as the GST 4-4-catalyzed reaction with 4-substituted 1-chloro-2-nitrobenzenes depend on  $\sigma_p^-$  in a similar way.

In a previous study, the  $k_s$  and  $k_{cat}/K_m$  values of the base- and GST 4-4-catalyzed GSH conjugation of 2-substituted 1-chloro-4-nitrobenzenes (**1a–10a**) were correlated with  $\sigma_p$  (21). From the different  $\rho$  values in these equations and additional regression analyses it was concluded that the rate-limiting step in the GSH conjugation of 2-substituted 1-chloro-4-nitrobenzenes are different for the base-catalyzed and the GST 4-4-catalyzed reactions (21). In the present study, however, no significant difference in dependence on electronic properties of the *para* substituents of 4-substituted 1-chloro-2-nitrobenzenes is observed between the base- or GST 4-4-catalyzed GSH conjugation reactions (Figure 6). Although both types of substrates (**1a–10a** and **1b–12b**) are conjugated to GSH via an identical S<sub>N</sub>Ar mechanism, the nature and position of the substituents apparently differentially influence the GSH conjugation rate and, by inference, also the transition states.

After multiple-regression analyses of  $\log k_{cat}/K_m$  and  $\log k_s$  of the 4-substituted 1-chloro-2-nitrobenzenes (**1b–12b**) with all eight physicochemical and all five computer-calculated parameters, only one significant correlation was found, i.e., between  $\log k_{cat}/K_m$  and the charge on the *o*-NO<sub>2</sub> substituent of the substrates and  $\sigma_p^-$ :

$$\log k_{cat}/K_m = -24.47(\pm 4.41)(\text{charge } o\text{-NO}_2) + 3.93(\pm 0.28)\sigma_p^- - 8.63(\pm 0.84) \quad (8)$$

$r = 0.993 \quad s = 0.125 \quad n = 6$

The correlation coefficient with the single parameter  $\sigma_p^-$  was significantly lower, 0.913, and the single regression with the charge on *o*-NO<sub>2</sub> showed no significant correlation ( $t = -0.18$ ). Equation 8 implies that when the  $\sigma_p^-$  increases and the charge on the *o*-NO<sub>2</sub> substituent becomes more negative, the  $k_{cat}/K_m$  will increase. The fact that this correlation was only observed for the GST 4-4-catalyzed GSH conjugation and not for the base-

catalyzed reaction, suggests that there is a unique interaction between the *o*-NO<sub>2</sub> substituent and an amino acid in the active site of GST 4-4. This interaction could be of electronic nature, giving an extra stabilization during formation of the Meisenheimer intermediates. This observation confirms the previously proposed interaction between the 2-substituents of 2-substituted 1-chloro-4-nitrobenzenes (IS<sub>2</sub>) and a Lewis acidic amino acid in the active site of GST 4-4 (*p*IS<sub>2</sub>) (15).

**Extension of the Substrate Model for GST 4-4. Description of the Substrate Model for GST 4-4.** On the basis of the regio- and stereoselective GST 4-4-catalyzed GSH conjugation reactions of 20 substrates [aromatic diol epoxides, pyrene oxide, (aza)phenanthrene oxides, and aromatic chlorides (i.e., substrates **1a–5a**, **9a**, **10a**, **4b**, and **6b**)], a substrate model has recently been developed which comprises the main structural characteristics of substrates for GST 4-4, using benzo[*a*]pyrene 7(*R*),8(*S*)-diol 9(*S*),10(*R*)-epoxide (BPDE) as a template (Figure 1) (15). Several as yet hypothetical structural elements in the active site of GST 4-4 have been indicated: a flat aromatic region responsible for orientation and stabilization of some substrates (*p*IS<sub>4</sub>) and three other interaction sites consisting of Lewis acid amino acids (*p*IS<sub>1</sub>, *p*IS<sub>2</sub>, and *p*IS<sub>3</sub>) (Figure 1). This substrate model appeared to be useful to rationalize the stereo- and regioselective GSH conjugation of a number of substrates by fitting them in the model (styrene oxides, stilbene oxides, 2-cyano-1,3-dimethyl-1-nitrosoguanidine, and *para*-substituted 4-phenyl-3-buten-2-ones). Moreover, recently a protein homology model for rat GST 4-4 was developed (42), and in combination with the substrate model for GST 4-4, various amino acids in or near the active site could be indicated which might be responsible for binding and/or activation of substrates.

**Addition of 2-Substituted 1-Chloro-4-nitrobenzenes to the Substrate Model.** Like the *o*-methyl ester- and *o*-butyl ester-substituted 1-chloro-4-nitrobenzenes (**4a** and **5a**, respectively) and the *o*-benzophenone analogue **3a** (15), substrate **6a** could not be fitted on BPDE in its minimal energy conformation, i.e., in which the *o*-carbonyl oxygen atom lies approximately in the plane of the aromatic ring. Therefore, these substrates were fitted alternatively onto the BPDE template by superimposing the sites of GS<sup>-</sup> attack and the carbonyl oxygen atom of the substituents onto IS<sub>2</sub>. The energy difference between the fitted and the minimal energy conformation of substrate **6a** was 5.53 kJ/mol, and the distance between the fitted atoms was 0.05 Å, indicating that this fit is acceptable. In this fit two of the methyl groups of the *tert*-butyl ester substituent are positioned on the border of an area where, in the substrate model as yet, no atoms of superimposed substrates were found. This observation, together with the fact that no measurable GSH conjugation of **6a** was found up to 300 μM when catalyzed by GST 4-4 while GSH conjugation of **6a** was observed when catalyzed by base (Table 2), suggests that steric restrictions in this area of the active site might be important. In a recent study, however, it was found that **6a** competitively inhibited the GST 4-4-catalyzed GSH conjugation of substrate **7a** with a  $K_i$  of 32 μM, indicating that **6a** binds to the active site with a relatively high affinity.<sup>2</sup> This suggests that there are no steric restrictions in the binding of **6a** to GST 4-4.

<sup>2</sup> E. M. van der Aar *et al.*, manuscript in preparation.

Substrate **7a** was fitted as well onto BPDE in its minimal energy conformation by superimposing the sites of  $\text{GS}^-$  attack on one hand and the N-atom of the *o*-CN substituent onto  $\text{IS}_2$  on the other hand. The distance between the fitted atoms was 0.13 Å, which is indicative for an acceptable fit. The *o*- $\text{CF}_3$  analogue **8a** was also fitted onto the template molecule in its minimal energy conformation. The sites of  $\text{GS}^-$  attack were superimposed, and one of the F atoms of  $\text{CF}_3$  was fitted onto  $\text{IS}_2$ , leading to small distances between the fitted atoms (0.05 Å).

**Addition of 4-Substituted 1-Chloro-2-nitrobenzenes to the Substrate Model.** For the fitting of 4-substituted 1-chloro-2-nitrobenzenes onto the template molecule BPDE, the respective sites of attack by GSH were matched and one of the oxygen atoms of the *o*- $\text{NO}_2$  substituent were fitted onto  $\text{IS}_2$ . The fits were performed with the minimal energy conformations of the 4-substituted 1-chloro-2-nitrobenzenes, and the distance between the fitted atoms was 0.11 Å. The methyl and *tert*-butyl ester analogues **4b** and **6b** were previously used to probe the steric restrictions of the active site of GST 4-4 (15). Substrate **4b** appeared to conjugate well to GSH, while for **6b** no measurable GSH conjugation was observed up to 300  $\mu\text{M}$  (Table 2). It was concluded that large bulky substituents at the position *para* relative to  $\text{C}_1$  cannot be accommodated in the active site of GST 4-4 (15).

The 4-halogen-substituted substrates **8b**, **9b**, and **10b** all fitted perfectly in the substrate model. No parts of the *para* substituents were crossing areas, described by the substrate model, and on the basis of their electron-withdrawing capacity they should conjugate to GSH when catalyzed by GST 4-4. Substrates **9b** and **10b**, however, showed no measurable GSH conjugation, which is probably due to the low extinction coefficients of the corresponding GS-conjugates as discussed before and not to steric restrictions (Br and  $\text{CF}_3$  have similar sizes,  $r_{\text{vdw}} = \pm 1.85$  Å).

Substrates **2b** and **5b**, similar to **4b** as previously described, can be fitted in two conformations (see Figure 2A and 2B) and apparently, because of their substantial GSH conjugation rate (Table 2), can be accommodated in either of the two conformations. For substrate **5b** several conformations are possible, because of the long flexible butyl chain. The lowest sterical hindrance, and by inference the lowest total energies, is observed in the extended conformations. Of the two extended conformations, the lowest energy conformations were calculated and used for a more detailed description of the substrate model for GST 4-4. Obviously, there is quite some space in the area *para* relative to the GSH conjugation site of 4-substituted 1-chloro-2-nitrobenzenes, because the long butyl ester part is not negatively influencing the GSH conjugation by GST 4-4. It cannot be excluded, however, that the GST protein accommodates the *n*-butyl chain in a folded conformation.

From the benzophenone- and phenyl ester-substituted compounds (**3b** and **11b**, respectively), which both have a high apparent affinity for GST 4-4 and a relatively high GSH conjugation rate (Table 2), four low-energy conformations were considered. Both substrates have two orientations of the carbonyl (Figure 2) and because of intramolecular sterical hindrance, the phenyl rings are positioned approximately  $+65^\circ$  and  $-65^\circ$  out of the aromatic plane for **3b**, while this is approximately  $+58^\circ$  and  $-58^\circ$  for **11b**. In Figure 7 are shown the fits of the four possible low energy conformations of **3b** and **11b**

onto BPDE. In the area *para* relative to the site of GSH attack ( $\text{C}_1$ ), a shaft becomes visible between the two mirrored conformations. In addition to extended alkyl chains at the *para* position, also relatively flat *para* substituents are obviously accommodated by GST 4-4.

To further examine the steric restrictions of *para* substituents for GST 4-4 and the importance of the above-mentioned shaft, the 3'-*tert*-butylphenyl ester-substituted compound **12b** was synthesized and tested as a substrate for GST 4-4. Up to a concentration of 300  $\mu\text{M}$ , no formation of GS-conjugate was measured. Electronic restrictions play no role because this compound was conjugated to GSH when catalyzed by base (Table 2). Eight low-energy conformations were fitted: the two orientations of the carbonyl (Figure 2), the phenyl ring twisted above and under the aromatic plane due to steric hindrance, and the *tert*-butyl substituent at both sides of the phenyl ring. In Figure 7 these eight conformations are fitted onto BPDE. It is clear that the *tert*-butyl group occupies the above mentioned shaft, and this might imply steric restrictions in this area of the active site of GST 4-4. To confirm this theory, the two low-energy conformations of the *tert*-butyl ester analogue **6b**, which was not conjugated to GSH up to 300  $\mu\text{M}$  by GST 4-4, were again fitted on the template (Figure 7). Also in this case, the bulky *tert*-butyl group occupies the defined shaft, and this might therefore also be a reason for **6b** not being a substrate for GST 4-4. These observations are in line with the previously discussed SAR equation 4. When the  $B_5$  Sterimol parameter becomes too large, as in the case of *tert*-butyl ester and *tert*-butyl phenyl ester substituents, the  $k_{\text{cat}}$  values become so low that they are no longer measurable.

We are aware of the fact that there might in principle be alternative binding modes of the 4-substituted 1-chloro-2-nitrobenzenes to the active site of GST 4-4. Several of these alternative binding modes have been considered, but the binding modes presented appeared to confirm the obtained results in the best possible way.

## Conclusions

In the present study, quantitative structure-activity relationships (SAR's) are described for base- and GST 4-4-catalyzed GSH conjugation of 4-substituted 1-chloro-2-nitrobenzenes (**1b**–**12b**). Eight physicochemical parameters, delineating electronic, steric, and lipophilic effects of the substituents, as well as five computer-calculated molecular parameters of the substrates (charge distributions and energy values) were used in the regression analyses with the kinetic parameters for the base- ( $k_s$ ) and GST 4-4-catalyzed ( $K_m$ ,  $k_{\text{cat}}$ ,  $k_{\text{cat}}/K_m$ ) reactions. The obtained SAR's were compared with corresponding SAR's for 2-substituted 1-chloro-4-nitrobenzenes (**1a**–**10a**). From a previous study, it appeared that the  $k_s$  and  $k_{\text{cat}}/K_m$  values of the base- and GST 4-4-catalyzed GSH conjugation of 2-substituted 1-chloro-4-nitrobenzenes depend differentially on the electronic properties of the 2-substituents. This suggested that these substrates are conjugated to GSH via different rate-limiting transition states when catalyzed by base or GST 4-4 (21). In the present study, however, the base- and GST 4-4-catalyzed GSH conjugation of 4-substituted 1-chloro-2-nitrobenzenes showed no significant differences in the dependence on the electronic properties of the substituents. This indicates that the position of the substituents relative to the reaction center and their electron-withdrawing

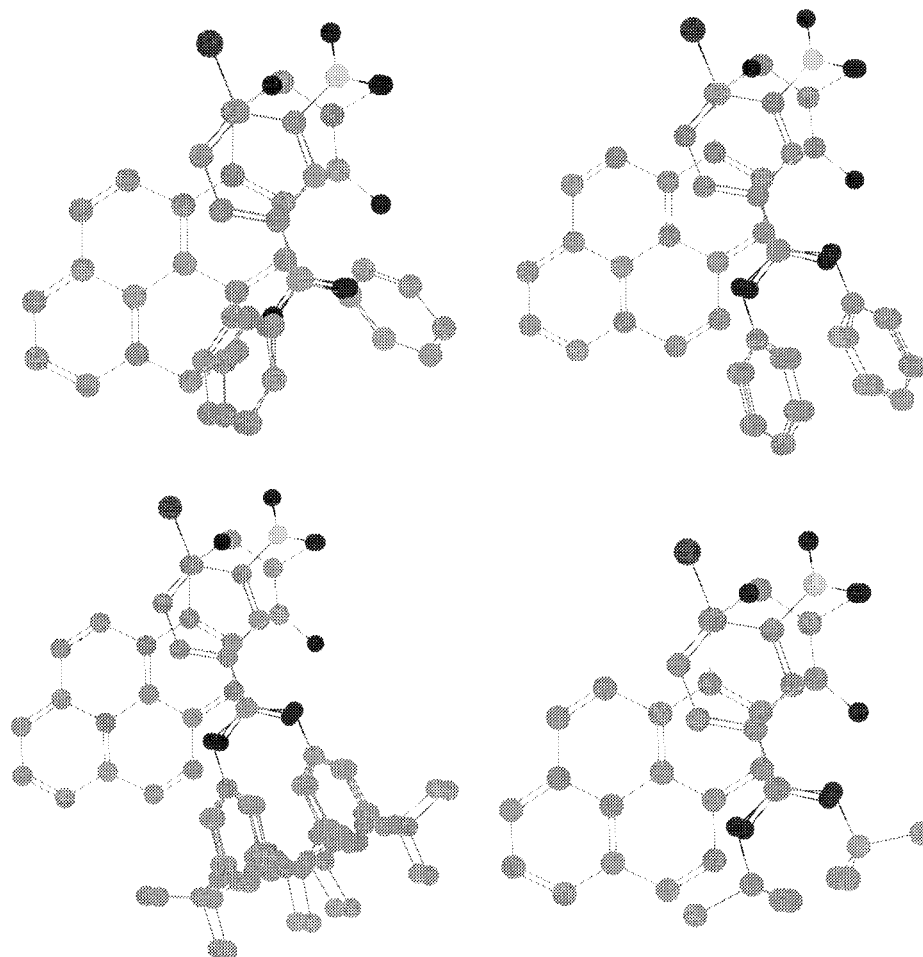


**Figure 7.** Fits of 4-substituted 1-chloro-2-nitrobenzenes onto the template molecule BPDE: three conformations of **3b** (upper left), four conformations of **11b** (upper right), eight conformations of **12b** (lower left), and two conformations of **6b** (lower right). Hydrogen atoms have been omitted.

capacity determine whether the rate-limiting transition state for the base-catalyzed nucleophilic aromatic substitution reaction is the same as for the GST 4-4-catalyzed reaction.  $\log k_s$ ,  $\log k_{cat}$ , and  $\log k_{cat}/K_m$  of the GSH conjugation of 4-substituted 1-chloro-2-nitrobenzenes (**1b**–**12b**) correlated well with the Hammett  $\sigma_p$  constant, corrected for through resonance ( $\sigma_p^-$ ), while the corresponding parameters of the 2-substituted 1-chloro-4-nitrobenzenes (**1a**–**10a**) did not. The process of through resonance is obviously of more importance in the GSH conjugation of 4-substituted 1-chloro-2-nitrobenzenes than of 2-substituted 1-chloro-4-nitrobenzenes, because in the latter series of substrates this process is probably not efficient, due to steric hindrance in the Meisenheimer intermediates between the *ortho* substituent and the Cl atom at C<sub>1</sub>.  $\log k_{cat}$  of GST 4-4 for the GSH conjugation of 2-substituted 1-chloro-4-nitrobenzenes correlated highly with the charge on the *p*-NO<sub>2</sub> substituent of these substrates, which appeared to be an indirect parameter for the electron-withdrawing capacity of the 2-substituents, corrected for steric influences ( $\sigma_o$ ).

Multiple-regression analyses with  $k_{cat}$  and  $k_{cat}/K_m$  for the GSH conjugation of 4-substituted 1-chloro-2-nitrobenzenes showed that, besides electronic effects, also steric ( $L$  and  $B_5$ ) and lipophilic ( $f$ ) factors of the substituents play a role. The lipophilicity of the *para* substituents, for example, should not be too high, because if it is, the GSH conjugation rate will be low.

The 4-substituted 1-chloro-2-nitrobenzenes were also used to refine the substrate model for GST 4-4, recently

described by De Groot *et al.* (15). Addition of these substrates gave more detailed information about the steric restrictions of substrates of GST 4-4 and by inference about the active site of GST 4-4. For the substrates with relative bulky substituents, *tert*-butyl ester and 3'-*tert*-butylphenyl ester, GSH conjugation was observed when catalyzed by base but not by GST 4-4. These compounds were fitted in the substrate model and appeared to occupy an area in the substrate model which can be assigned as a "forbidden area".

## References

- (1) Commandeur, J. N. M., Stijntjes, G. J., and Vermeulen, N. P. E. (1995) Enzymes and transport systems involved in the formation and disposition of glutathione *S*-conjugates. *Pharmacol. Rev.* **47**, 271–330.
- (2) Armstrong, R. N. (1991) Glutathione *S*-transferases: Reaction mechanism, structure, and function. *Chem. Res. Toxicol.* **4**, 131–140.
- (3) Mannervik, B., Ålin, P., Guthenberg, C., Jenssen, H., Tahir, M. K., Warholm, M., and Jornvall, H. (1985) Identification of three classes of glutathione transferases common to several mammalian species. Correlation between structural data and enzymatic properties. *Proc. Natl. Acad. Sci. U.S.A.* **82**, 7202–7206.
- (4) Meyer, D. J., Coles, B., Pemble, S. E., Gilmore, K. S., Fraser, G. M., and Ketterer, B. (1991) Theta, a new class of glutathione transferases purified from rat and man liver. *Biochem. J.* **274**, 409–414.
- (5) Buetler, T. M., and Eaton, D. L. (1992) Glutathione *S*-transferases: Amino acid sequence comparison, classification and phylogenetic relationship. *Environ. Carcinog. Ecotoxicol. Rev.* **C10**, 181–203.

- (6) Johnson, W. W., Liu, S. X., Ji, X. H., Gilliland, G. L., and Armstrong, R. N. (1993) Tyrosine-115 participates both in chemical and physical steps of the catalytic mechanism of a glutathione *S*-transferase. *J. Biol. Chem.* **268**, 11508–11511.
- (7) Ploemen, J. H. T. M., Johnson, W. W., Jespersen, S., Vanderwall, D., Van Ommen, B., Van der Greef, J., Van Bladeren, P. J., and Armstrong, R. N. (1994) Active-site tyrosyl residues are targets in the irreversible inhibition of a class mu glutathione transferase by 2-(*S*-glutathionyl)-3,5,6-trichloro-1,4-benzoquinone. *J. Biol. Chem.* **269**, 26890–26897.
- (8) Zhang, P., Liu, S., Shan, S., Ji, X., Gilliland, G. L., and Armstrong, R. N. (1992) Modular mutagenesis of exons 1, 2, and 8 of a glutathione *S*-transferase from the Mu class. Mechanistic and structural consequences for chimeras of isoenzyme 3-3. *Biochemistry* **31**, 10185–10193.
- (9) Katusz, R. M., Bono, B., and Colman, R. F. (1992) Identification of Tyr<sup>115</sup> labeled by *S*-(4-bromo-2,3-dioxobutyl)glutathione in the hydrophobic substrate binding site of glutathione *S*-transferase, isoenzyme 3-3. *Arch. Biochem. Biophys.* **298**, 667–677.
- (10) Cooke, R. J., Björnstedt, R., Douglas, K. T., McKie, J. H., King, M. D., Coles, B., Ketterer, B., and Mannervik, B. (1994) Photoaffinity labelling of the active site of the rat glutathione transferases 3-3 and 1-1 and human glutathione transferase A1-1. *Biochem. J.* **302**, 383–390.
- (11) Penington, C. J., and Rule, G. S. (1992) Mapping the substrate-binding site of a human class mu glutathione transferase using nuclear magnetic resonance spectroscopy. *Biochemistry* **31**, 2912–2920.
- (12) Reinemer, P., Dirr, H. W., Ladenstein, R., Schäffer, J., Gallay, O., and Huber, R. (1991) The three-dimensional structure of class  $\pi$  glutathione *S*-transferase in complex with glutathione sulfonate at 2.3 Å resolution. *EMBO J.* **10**, 1997–2005.
- (13) Ji, X., Zhang, P., Armstrong, R. N., and Gilliland, G. L. (1992) The three-dimensional structure of glutathione *S*-transferase from the Mu gene class. Structural analysis of the binary complex of isoenzyme 3-3 and glutathione at 2.2-Å resolution. *Biochemistry* **31**, 10169–10184.
- (14) Sinning, I., Kleywegt, G. J., Cowan, S. W., Reinemer, P., Dirr, H. W., Huber, R., Gilliland, G. L., Armstrong, R. N., Ji, X. H., Board, P. G., Olin, B., Mannervik, B., and Jones, T. A. (1993) Structure determination and refinement of human-alpha class glutathione transferase A1-1, and a comparison with the Mu-class and Pi-class enzymes. *J. Mol. Biol.* **232**, 192–212.
- (15) De Groot, M. J., Van der Aar, E. M., Nieuwenhuizen, P. J., Van der Plas, R. M., Donné-Op den Kelder, G. M., Commandeur, J. N. M., and Vermeulen, N. P. E. (1995) A predictive substrate model for rat glutathione *S*-transferase 4-4. *Chem. Res. Toxicol.* **8**, 649–658.
- (16) Adang, A. E. P., Moree, W. J., Brussee, J., and Mulder, G. J. (1991) Inhibition of glutathione *S*-transferase 3-3 by glutathione derivatives that bind covalently to the active site. *Biochem. J.* **278**, 63–68.
- (17) Danielson, U. H., Esterbauer, H., and Mannervik, B. (1987) Structure–activity relationships of 4-hydroxyalkenals in the conjugation catalysed by mammalian glutathione transferases. *Biochem. J.* **247**, 707–713.
- (18) Rietjens, I. M. C. M., Soffers, A. E. M. F., Hooiveld, G. J. E. J., Veeger, C., and Vervoort, J. (1995) Quantitative structure–activity relationships based on computer calculated parameters for the overall rate of glutathione *S*-transferase catalyzed conjugation of a series of fluoronitrobenzenes. *Chem. Res. Toxicol.* **8**, 481–488.
- (19) Soffers, A. E. M. F., Ploemen, J. H. T. M., Moonen, M. J. H., Wobbles, T., Van Ommen, B., Vervoort, J., Van Bladeren, P. J., and Rietjens, I. M. C. M. (1996) Regioselectivity and quantitative structure–activity relationships for the glutathione conjugation of a series of fluoronitrobenzenes by purified glutathione *S*-transferase enzymes from rat and man. *Chem. Res. Toxicol.* **9**, 638–646.
- (20) Van der Aar, E. M., Buikema, D., Commandeur, J. N. M., Te Koppele, J. M., Van Ommen, B., Van Bladeren, P. J., and Vermeulen, N. P. E. (1996) Enzyme kinetics and substrate selectivities of rat glutathione *S*-transferase isoenzymes towards a series of new 2-substituted 1-chloro-4-nitrobenzenes. *Xenobiotica* **26**, 143–155.
- (21) Van der Aar, E. M., De Groot, M. J., Bijloo, G. J., Van der Goot, H., and Vermeulen, N. P. E. (1996) Structure–activity relationships for the glutathione conjugation of 2-substituted 1-chloro-4-nitrobenzenes by rat glutathione *S*-transferase 4-4. *Chem. Res. Toxicol.* **9**, 527–534.
- (22) Hammond, G. S., and Modic, F. J. (1953) Aromatic nitration. I. The ultraviolet spectra of aromatic nitro compounds in sulfuric acid. *J. Am. Chem. Soc.* **75**, 1385–1388.
- (23) Chemical Design Ltd. (1993) *ChemX*, Version January 1993.
- (24) Department of Chemistry Columbia University (1994) *Macro-model*, Version 4.5.
- (25) Weiner, S. J., Kollman, P. A., Case, D. A., Singh, U. C., Ghio, C., Alagona, G., Profeta, S., and Weiner, P. (1984) A new force field for molecular mechanical simulation of nucleic acids and proteins. *J. Am. Chem. Soc.* **106**, 765–784.
- (26) Weiner, S. J., Kollman, P. A., Nguyen, D. T., and Case, D. A. (1986) An all-atom force field for simulations of proteins and nucleic acids. *J. Comput. Chem.* **7**, 230–252.
- (27) Department of Chemistry Columbia University (1994) *Batchmin*, Version 4.0.
- (28) Dupuis, M., Spangler, D., and Wendoloski, J. (1980) *NRCC Program No. QG01 (GAMESS)*.
- (29) Guest, M. F., van Lenthe, J. H., Kendrick, J., Schoffel, K., Sherwood, P., Harrison, R. J., with contributions from: Amos, R. D., Buenker, R. J., Dupuis, M., Handy, N. C., Hillier, I. H., Knowles, P. J., Bonacic-Koutecky, V., von Niessen, W., Saunders, V. R., and Stone, A. J. (1993) *GAMESS-UK*, IBM RS6000 Version 2.1.
- (30) Hehre, W. J., Stewart, R. F., and Pople, J. A. (1969) Self-consistent molecular orbital methods. I. Use of Gaussian expansions of Slater-type atomic orbitals. *J. Chem. Phys.* **51**, 2657–2664.
- (31) Stone, A. J. (1981) Distributed multipole analysis, or how to describe a molecular charge distribution. *Chem. Phys. Lett.* **83**, 233–239.
- (32) Binkley, J. S., Pople, J. A., and Hehre, W. J. (1980) Self consistent molecular orbital methods. 21. Small split-valence basis sets for first-row elements. *J. Am. Chem. Soc.* **102**, 939–947.
- (33) Gordon, M. S., Binkley, J. S., Pople, J. A., Pietro, W. J., and Hehre, W. J. (1982) Self consistent molecular orbital methods. 22. Small split-valence basis sets for second-row elements. *J. Am. Chem. Soc.* **104**, 2797–2803.
- (34) Silipo, C., and Vittoria, A. (1990) Three-dimensional structure of drugs. In *Comprehensive medicinal chemistry* (Hansch, C., Sammes, P. G., and Taylor, J. B., Eds.) Vol. 4, pp 153–204, Pergamon Press, Oxford.
- (35) Rekker, R. F., and Mannhold, R. (1992) *Calculation of drug lipophilicity. The hydrophobic fragmental constant approach*, VCH, Weinheim, Germany.
- (36) Hansch, C., and Leo, A. (1979) *Substituent constants for correlation analysis in chemistry and biology*, Wiley, New York.
- (37) Hammett, L. P. (1940) *Physical Organic Chemistry*, McGraw-Hill, New York.
- (38) Swain, C. G., and Lupton, E. C. (1968) Field and resonance components of substituent effects. *J. Am. Chem. Soc.* **90**, 4328–4337.
- (39) Miller, J. (1968) in *Reaction mechanisms in organic chemistry* (Eaborn, C., and Chapman, N. B., Eds.) Vol. 8, pp 137–179, Elsevier, New York.
- (40) Keen, J. H., Habig, W. H., and Jakoby, W. B. (1976) Mechanism for the several activities of the glutathione *S*-transferases. *J. Biol. Chem.* **251**, 6183–6188.
- (41) Chen, W.-J., Graminski, G. F., and Armstrong, R. N. (1988) Dissection of the catalytic mechanism of isoenzyme 4–4 of glutathione *S*-transferase with alternative substrates. *Biochemistry* **27**, 647–654.
- (42) De Groot, M. J., Vermeulen, N. P. E., Mullenders, D. L. J., and Donné-Op den Kelder, G. M. (1996) A homology model for rat Mu class glutathione *S*-transferase 4-4. *Chem. Res. Toxicol.* **9**, 28–40.
- (43) Habig, W. H., and Jakoby, W. B. (1981) Assay for differentiation of glutathione *S*-transferases. *Methods Enzymol.* **77**, 398–405.

TX960137W